# Pseudonajide is an antibiotic peptide derived from snake venom that alter cell wall and membrane integrity interfering on biofilm formation.

**Rafael Schneider**
Institut de Genetique et Developpement de Rennes
**Muriel Primon-Barros**
Universidade Federal do Rio Grande do Sul
**Rafael Gomes Von Borowski**
Institut de Genetique et Developpement de Rennes
**Sophie Chat**
Institut de Genetique et Developpement de Rennes
**Reynald Gillet**
Institut de Genetique et Developpement de Rennes
**Alexandre José Macedo** (alexandre.macedo@ufrgs.br)
Universidade Federal do Rio Grande do Sul Pro-Reitoria de Pesquisa

**Research article**

**Keywords:** Antimicrobial peptide; Staphylococcus epidermidis; biofilm; snake venom; pseudonajide.

**Posted Date:** November 14th, 2019

**DOI:** https://doi.org/10.21203/rs.2.17309/v1



**Version of Record:** A version of this preprint was published on August 3rd, 2020. See the published version at https://doi.org/10.1186/s12866-020-01921-5.

# Abstract

Background The increase of bacterial resistance phenotype cases is a global health problem. New strategies in scientific community must be explored in order to create new treatment alternatives. Animal venoms are a good source for antimicrobial peptides (AMPs), which are excellent candidates for new antimicrobial drug development. These molecules have highly diverse targets in prokaryotic cells, making resistance phenotype development more difficult. Results In this study we present a peptide of just 11 amino acids which has antimicrobial and antibiofilm activity against Staphyloccocus epidermidis. Named pseudonajide, it is derived from Pseudonaja textilis venom. Pseudonajide was selected based on the sequence alignments of various snake venom peptides that displayed activity against bacteria. Several concentrations of pseudonajide were tested in antibiofilm activity essay, it was detected that 25 μM was the best minimal concentration for biofilm inhibiting activity. Microscopy analysis demonstrates that pseudonajide interacts with the bacterial cell envelope, disrupting the cell wall and membrane leading to morphological defects in prokaryotes. Conclusions Our results suggest that pseudonajide's positives charges interacts with negative charged cell wall components of S. epidermidis. Leading to cell damage and biofilm formation inhibition.


# Background

Animal venoms are complex mixtures of protein and peptide toxins, enzymes, and other compounds. Because they are both potent and interact specifically with the cell wall and membrane compounds of different cells, venom constituents are attractive candidates for the development of novel therapeutics and pesticides (1), although they remain largely unexplored. These rich molecule blends contain many antimicrobial peptides (AMPs) (2), and AMP sequences are available from the Antimicrobial Peptide Database (APD) databank (http://aps.unmc.edu/AP) (3). AMPs are very promising and are sure to be innovative additions to the arsenal of weapons against resistant bacteria (4, 5).

AMPs have complex and wide-ranging mechanisms of action. They can directly target bacterial membranes, damaging cell integrity and consequently causing osmotic imbalance. They can also disrupt macromolecular synthesis, interfering in cell wall biosynthesis (6). Due to this complexity and the wide scale of their target interactions, resistance to such molecules seems to arise less commonly than with conventional antibiotics (7). However, not much investigation has been done on their mechanisms of action in bacterial biofilm (8). Biofilms are well-organized microbial associations normally attached to abiotic or biotic surfaces. Their structure is characterized by matrix accumulation, and the formation process consists of several stages. The first step is microbial cell adherence, which is dependent on hydrophobicity, cell wall teichoic acids, and other proteins related to the cell wall. Microcolonies then form and mature, with establishment and maintenance of the structure occurring by both matrix and cell accumulation (9), followed by dispersion, the final step of biofilm formation (10). There are several advantages to this form (11): a biofilm community is difficult to treat due to the physical barrier against antibiotics and immune system factors (12); and the structure is related to much higher antimicrobial resistance (13). In most cases, the first treatment option for biofilm on medical devices is removal of the

devices themselves, leading to increases in both patient suffering and health system financial expenditures (14).

*Staphylococcus epidermidis* is a commensal microorganism widely present on human skin (15), making this species one of the main causes of infections related to biofilm formation in medical devices (16, 17). Indeed, biofilm formation is the most prominent virulence factor during the pathogenesis of *S. epidermidis* (18). Commensal skin flora or hospital bacteria can adhere to a foreign body, replicate, and form biofilm, which can then for instance invade peri-implant tissue, causing serious infection (14, 19). *S. epidermidis* infections on central venous catheters occur annually in approximately 80,000 cases in the United States, leading to several blood infection cases (20, 21). Furthermore, *S. epidermidis* is related to 17-39% of infections in prosthetic valve endocarditis (22). Due to this prevalence, and the global increase in bacterial resistance of all kinds, the search for new molecules to treat bacterial infection is extremely urgent (23). Here, we present pseudonajide, a synthetic peptide made up of 11 amino acids and derived from *Pseudonaja textilis* snake venom. It possesses antimicrobial and antibiofilm activity against *S. epidermidis*, and our results suggest that pseudonajide acts on the cell wall and membrane compounds of that bacteria, quite quickly and at low doses.

# Results

### 2.1 Sequence alignment and peptide selection

The sequences of seven snake venom peptides having related antimicrobial activities (2) deposited in the Antimicrobial Peptide Database (APD) website (http://aps.unmc.edu/AP) were aligned using Clustal X software (24). After alignment analysis of the common sequences of these seven peptides, 17 small peptides were synthesized (Fig. 1).

### 2.2 Peptides 1, 2, and 3 have antibiofilm activity in *epidermidis*

The first aim of this work was to perform a screening for antibiofilm activity in 17 small peptides derived from snake venom. For that, we chose two different species of bacteria, one Gram-negative (*Pseudomonas aeruginosa* PAO1), and one Gram-positive (*S. epidermidis* ATCCC 35984). This selection was based on their biofilm production capabilities, and both strains are known to be good models for the study of biofilm formation and structures (9, 25). For screening, a crystal violet stain protocol was used with or without different concentrations of peptides. No effects were detected on biofilm formation in *P. aeruginosa* (Fig. S2). On the other hand, peptides 1, 2, and 3 demonstrated strong activity on the *S. epidermidis* biofilm. After 24 hours of exposition to different concentrations, there was a considerable reduction in biofilm mass (Fig. 2A). At a concentration of 100 µM, the biofilm mass was reduced by 77%, 95%, and 78% for peptides 1 to 3, respectively (Fig. 2A).

Peptide 2 demonstrated greater antibiofilm activity than peptides 1 and 3. The considerable reduction of 63% of the biofilm mass in the presence of 25 µM of peptide 2 led us to select that particular molecule at that specific concentration for the following experiments. We named the peptide “pseudonajide” after the

name of the snake it was derived from, *Pseudonaja textilis*. In order to test its biofilm eradication activity, we precultured *S. epidermidis* cells for 24 h adding pseudonajide to pre-formed biofilm and incubating for another 24 h. The final quantification of biofilm mass showed a reduction of about 30% in the presence of the molecule (Fig. 2B).

### 2.3 Pseudonajide has antimicrobial activity against *epidermidis*

We decided to test the antimicrobial activity over a shorter period of time, because no difference had been observed after 24 h. Growth and colony-forming unit (CFU) tests were performed. Cells were incubated in the same conditions as for the antibiofilm tests, with or without 25 µM pseudonajide. After 1, 2, 4, and 24 h incubation, we measured the optical density at 600 nm ($OD_{600}$) and assessed the CFU counts. Fig. 3 shows clearly that the molecule's presence causes a huge decrease in bacterial growth as compared to the control. The same result was seen in the CFU experiments. After 1, 2, or 4 h incubation with pseudonajide, the number of viable cells vastly decreases as compared to the control conditions.

### 2.4 Pseudonajide binds to the cell wall and membrane, causing permeabilization

To better understand pseudonajide's binding site, we synthesized peptides tagged with *fluorescein* isothiocyanate (FITC), and then performed confocal microscopy. Cells were incubated with 25 µM FITC-tagged pseudonajide for 1, 4, or 24 h. After incubation, confocal microscopy showed that the molecule is located around or inside the bacterial cell, but not in the biofilm matrix (Fig. 4). Another important finding was the reduction of fluorescent cells over time, with decreased peptide-tagged cell counts after 4 and 24 h incubation.

To confirm that the interaction occurs between pseudonajide and *S. epidermidis* cell walls and membranes, we did LIVE/DEAD experiments. Because it was demonstrated that propidium ions can enter on cell with high membrane potential (26). Cells were cultured for 4 h with or without 25 µM pseudonajide. Confocal microscopy image analysis demonstrates an increase in cell death when in the presence of pseudonajide. Moreover, statistical analysis shows that there is a significant decrease in the number of impermeable cells when the peptide is present (Fig. 5). These data suggest that pseudonajide are interfering on cell walls and membranes integrity.

### 2.5 Pseudonajide damages *epidermidis* cell walls and membranes

To check for morphological changes in *S. epidermidis* cells after exposure to the peptide, microscopy experiments were then performed after 1, 4, and 24 h incubation with or without 25 µM pseudonajide. We chose to approach this in two distinct ways, using both scanning electron microscopy (SEM) and transmission electron microscopy (TEM). The SEM experiments were performed by culturing the cells in the same conditions as before, with plastic slides added to the culture well for cell adherence. Our most notable result was that after 4 and 24 h incubation, cell adhesion was much weaker when cultured with the peptide, although no difference was observed after just 1 h (Fig. 6). Another important characteristic we noted was that several cells exposed to this molecule had a shrunken morphology and were smaller

than non-exposed cells (Fig. 6, white arrows). Again, this morphology was only noted after 4 and 24 h incubation. A final point that must be highlighted is that some extravasated material is present surrounding the shrunken cells, and this can be seen in the same figure in the cells that have arrows. None of these characteristics were seen in the control.

After the SEM experiments and analysis, two questions remained unanswered: how does pseudonajide cause cells shrink? Is there any damage to the cell walls or to the membrane? To address these questions, we performed TEM. This imaging method allows for the analysis of cell component ultrastructures and thus the analysis of cell wall and membrane integrity. Analysis of the resulting images demonstrated disrupted cells after pseudonajide exposition (Fig. 7, dark arrows). Specifically, after 4 and 24 h of peptide exposition, the cell wall is not intact, and the cell sizes are completely different than those of the control. Moreover, in the peptide-exposed cells, the material inside the cytoplasm is condensed (Fig. 7).

### 2.6 Pseudonajide increases the expression of genes coding for teichoic acid synthesis

The results obtained from microscopy analysis led us to hypothesize that pseudonajide acts on cell walls and membranes. Indeed, cationic peptides are known to be able to interact with the cell walls of Gram-positive bacteria (27) and to influence membrane fluidity when engaging with the phospholipid bilayer (28). One of the first molecules that is supposed to interact with cationic peptides is teichoic acid, a negatively charged molecule present in Gram-positive cell walls (29). To investigate this, real-time quantitative PCR tests were done, with *S. epidermidis* cultured in the same conditions as the previous experiments. However, due to pseudonajide's high antimicrobial activity, we decided to use a lower concentration. We therefore tested a series of dilutions ranging from 3 to 100 µM of the molecule at 4 h incubation. We found that a concentration of 6.25 µM is enough to inhibit about 50% of growth as compared to the control (Fig. 8A). To investigate the relative expression levels of genes when bacterial cells are cultured in subtoxic concentrations of this peptide, we selected three genes that code for teichoic acid molecules. By testing these, we were able to clearly see that cells cultured in the presence of 6.25 µM peptide had higher expression levels of UgtP, LtaA, and LtaS genes (Fig. 8B). These results led us to hypothesize that pseudonajide interacts with teichoic acid in the *S. epidermidis* cell wall, causing a strong interaction with this structure, leading to cell permeability. The same extracted RNA was used for biofilm-related gene expression analysis. We chose nine genes related to biofilm formation for expression analysis: *AtleE, agrC, aap, EmbP, icaA, leuA, saeR, saeS,* and *sarA*. No significant differences in expression were observed under control and peptide conditions for these nine genes (Fig. 8C).

One of main challenges in the development of antimicrobial peptides is their potential toxicity to human cells (30, 31). We therefore performed toxicity tests using seven human cell lines: HuH7 (hepatocellular carcinoma); Caco-2 (colorectal adenocarcinoma); MDA-MB231 (breast adenocarcinoma); HCT116 (colorectal carcinoma); PC3 (prostatic adenocarcinoma); NCL-H727 (lung carcinoma); and MCF7 (breast cancer). After 24 h incubation in a concentration of 25 µM pseudonajide, there was no decrease in the

living cell counts as compared to the control conditions (Fig. 9), demonstrating that pseudonajide is not cytotoxic to human cells.

# Discussion

Antimicrobial peptides are promising molecules in the fight against bacterial resistance (32). Since AMPs can interact with a large variety of cell targets, they have an advantage in the fight against the production of bacterial resistance phenotypes (33). We demonstrate here that an 11-amino-acid peptide derived from *P. textilis* snake venom possesses antimicrobial activity against *S. epidermidis*. Our first goal during the screening was to find new molecules with antibiofilm activity. However, when we investigated the mechanism of action of peptide 2, we found that it acts directly on the bacterial cell, and not in the biofilm matrix. This led us to investigate its antimicrobial activity, the molecule's cellular binding site, as well as the bacterial molecules which might interact with this newly identified peptide.

To analyze the effects of pseudonajide on *S. epidermidis* cells, we performed growth curve and CFU experiments using a concentration of the peptide of 25 µM. We began by investigating the peptide's effects in the early stages of interaction. In fact, it is possible to detect a great difference in the CFU counts after just 1, 2, and 4 h incubation, which is characteristic of a fast-action antibiotic. Moreover, biofilm eradication activity was detected (Fig. 2D), with around 30% lower biofilm mass as compared to the control conditions, possibly due to the ability of pseudonajide to kill the biofilm-forming bacteria. This shows that the peptide has a dual action, both antimicrobial and against biofilm formation. To discover the binding sites of pseudonajide, we produced an FITC-tagged molecule. After 1, 2, and 24 h interaction with bacterial cells, confocal microscopy demonstrated that pseudonajide interacts with the *S. epidermidis* cell envelope (Fig. 4). We can therefore conclude that the first bacterial cell interactions are with the cell envelope, and not with the biofilm matrix.

Based on their activities, AMPs can be divided into two main groups: they can act on the cell wall and disrupt the membrane, causing cell permeability; or they can have intracellular targets (34, 35). Even though cationic peptides can have different amino acid sequences, they still have similar characteristics which permit interaction with bacterial cell membranes. As described on the literature, most of the residues in AMPs are positively charged and some are hydrophobic, ensuring the AMPs amphipathic character (27, 36). In this work, structural analysis demonstrated that more than 50% of the amino acids which make up the peptide pseudonajide are positively charged (KRFKKFFMKLK). The position of methionine (M) seems to increase the antimicrobial/antibiofilm activity, and such a residue was not seen in peptides 1 (KRFKKFFKKVK) or 3 (KRFKKFFKKLK). The original peptide sequence that we based to synthesize pseudonajide was reported by Falcão's group, and belong to the vipericidins, a family of cathelicidin-related peptides derived from the venom glands of South American pit vipers. They described these vipericidins as having antimicrobial activities against different bacteria, including *S. aureus* and *P. aeruginosa* strains (37). Their activity is probably similar to the interactions we saw between pseudonajide and the *S. epidermidis* cell walls and membranes. AMPs bind preferentially to the cationic bacterial membrane instead of the zwitterionic membrane in mammalian cells (36). Moreover,

pseudonajide contains 36% hydrophobic amino acids, a characteristic which may explain its interactions with the bacterial cell membrane. Insertion of the peptide into the hydrophobic portion of the membrane seems to cause osmotic imbalance in the cell, which could lead to the shrunken cell morphology observed in the SEM (Fig. 6) and TEM (Fig. 7) analysis. It is important to note that in TEM, the defective cells have external material surrounding them. We hypothesize that this consists of extravasated DNA and disorganized peptidoglycan, but more tests are necessary to prove it. We also surmise that the smaller cells that can be observed are the same as those seen on FITC-tagged peptides with confocal microscopy. The green fluorescent cell sizes were all smaller than those of the non-fluorescent cells. In summary, pseudonajide acts on the cell envelope, inducing an osmotic imbalance which in turn causes a reduction in cell size, leading to cell death (Fig. 5).

The cell wall in Gram-positive bacteria is a complex network of molecules in a structure composed mainly of peptidoglycan and teichoic acids. Teichoic acids are negatively charged poly-glycerophosphate chains that can be linked to peptidoglycan or anchored to the cytoplasmic membrane (38, 39). Moreover, D-alanylation of lipoteichoic acid is said to promote protection against cationic AMPs in Gram-positive bacteria (40). In order to test this, we assessed the expression levels of genes coding for LTA assembly molecules, namely glycosyltransferase YgfP (UgtP), flippase LtaA, and lipoteichoic acid synthase LtaS (41). In *S. aureus,* lipoteichoic acid synthesis starts with YgfP, encoded by the *ugtP* gene. This protein synthesizes the glycolipid anchor Glc2-DAG from UDP-Glc and diacylglycerol (DAG). Glc2-DAG is translocated to the outside of the membrane by LtaA (41, 42), and elongation of the LTA chain is then promoted by LtaS (41, 43). Based on the literature and due to the physicochemical characteristics of teichoic acids, we speculated that pseudonajide must act on teichoic acids in the *S. epidermidis* cell wall. We detected increases in the expressions of all three tested genes when the cells were cultured in the presence of pseudonajide (Fig. 8B). These results reinforce our theory that pseudonajide binds to *S. epidermidis* lipoteichoic acids, probably causing cell wall disorganization in these bacteria (Fig. 10). The increased expression may well be a compensatory mechanism to protect against the presence of the peptide or even to preserve cell viability.

It was previously suggested that cationic antimicrobial peptides kill bacterial cells. They first interact with the membrane through electrostatic interactions (44), contacts which result in membrane disruption and cell death. Other peptides can cross the bacterial lipid bilayer without causing any damage to the cell membrane, but still inhibit intracellular functions, so they also eventually lead to bacteria death. Pseudonajide contains an amino acid sequence (KRFKKFFMKLK) that is part of a peptide isolated from *P. textilis* venom. Of the peptides we tested, pseudonajide has the best antibiofilm formation activity, at a sub-MIC concentration of just 6.25 uM (Fig. 2B), and the best eradication of established biofilm activity in the group (Fig. 2D). Several AMPs have been described as also having antimicrobial activity against Gram-negative bacteria. In the present work, we did not observe any antibiofilm or antimicrobial activity against *P. aeruginosa* (Fig. S2). It is possible that the short peptides tested here suffer from *P. aeruginosa* protease degradation (45, 46), as small peptides are typically more susceptible to proteases. The inhibition of LL-37's bactericidal activity by alginate and exopolysaccharides is another example of

antimicrobial peptide protection reported in this same pathogen. The inhibition occurs through LL-37 sequestration, which diminishes AMP concentrations at the target site (47).

We have observed  pseudonajide's dual activity, as it is both antimicrobial and also inhibiting *S. epidermidis* biofilm formation. Even though we did not see any alteration in the expression of biofilm-related genes when the peptide was present, we did observe biofilm eradication with reduction in mass (Fig. 2B). This decrease can be explained by several elements. One is the relationship between the cell wall teichoic and lipoteichoic acids and the processes of adhesion and biofilm formation (48). In *S. epidermidis,* cell wall teichoic acids seem to induce adhesion-immobilized fibronectin (49). Moreover, these types of molecules have been detected in the biofilm matrix of *S. epidermidis* (50). If pseudonajide mainly acts on teichoic and lipoteichoic acids, the reduction in adhesion could be one of the causes of both biofilm reduction and outright eradication. It is also important to emphasize the characteristics of cationic antibiofilm peptides, described by Von Borowski *et al.* (51). They showed that lysine (K) and phenylalanine (F) are the most frequently found amino acids in antibiofilm peptides, and this is clearly also the case for pseudonajide (KRFKKFFMKLK).

We have showcased here the promising activity of a synthetic peptide derived from *P. textilis* venom. Its dual action against *S. epidermidis* cells and its biofilm make pseudonajide a very promising molecule for new drug development, and this is reinforced by the fact that it has a short sequence. Shorter sequences are advantageous both for industry and antimicrobial peptide researchers, as they are easier to synthesize and cost less. Importantly, this facilitates future research into their structures and into ways to improve their efficiency.

# Methods

### 4.1 Bacterial strains and culture conditions

*S. epidermidis* ATCC 35984 was used to test the antimicrobial and antibiofilm activities of the peptides. Bacteria were grown in blood agar plates and cultured overnight at 37° C. Cell suspensions were prepared in a solution of 0.9% NaCl and adjusted to $OD_{600}$ for a final concentration of $\sim 10^8$ cells/ml. For microscopy analysis, pre-inoculum was made in tryptic soy broth (TSB, Merck), and adjusted to $OD_{600}$ for the same concentration of cells for all tests.

### 4.2 Tests on antimicrobial and antibiofilm activity

Serial dilution of peptides was performed in 96-well plates, going from 100 to 3.12 µM. Cell suspensions and TSB were added to the plates and a control was made with dimethyl sulfoxide (DMSO). Antibiofilm formation tests were performed with an adapted protocol (52), which it is described that  24 h of incubation is sufficient to determinate antibiofilm activity. The $OD_{600}$ was measured, then biofilm content accessed using the crystal violet protocol (53). Biofilm eradication test was performed supplementing 24 h pre-formed biofilm with a new culture broth, containing or not 25 µM of peptide. The plates were incubated for more 24 h followed by crystal violet protocol. The antimicrobial activity of pseudonajide

was analyzed using a concentration of 25 µM after 1, 2, 4, and 24 h incubation. After measuring the optical density, the supernatant was collected and diluted. A volume of 100 µl was plated in Luria broth agar plates. CFUs were counted after 24 h incubation. All experiments were performed at least three different times, each with three technical replicates.

### 4.3 Scanning electron microscopy

*S. epidermidis* was cultured in the same conditions as described previously, in the presence or absence of 25 µM pseudonajide. However, for this analysis, a plastic slide was placed inside each well, and these plates were incubated for 1, 4, and 24 h. After incubation, the plastic slides were washed three times with 0.9% NaCl solution and fixed overnight in fixation buffer (2.5% glutaraldehyde, 2% paraformaldehyde, 0.1 M sodium cacodylate) at 4° C. The adhered cells were then dehydrated with increasing concentrations of ethanol solutions. The images were obtained using a JSM-7100F scanning electron microscope (JEOL).

### 4.4 Transmission electron microscopy

Bacterial cells were cultured in 24-well plates in the presence or absence of 25 µM of pseudonajide. Cells were incubated for 1, 4, and 24 h. All of the content in the well was recovered, centrifuged at 12,000 xg, then washed with saline solution. Fixation was performed for 18 h at 4° C with a buffer (0.2 M sodium cacodylate, 16% paraformaldehyde, 25% glutaraldehyde, 75 mM lysine). Samples were then washed 4 times with a solution containing 0.1 M sodium cacodylate and 0.2 M sucrose. After each resuspension, samples were incubated for 10 min in this solution. Contrast was done for 1 h with a solution of 1% osmium tetroxide and 1.5% potassium ferrocyanure. Dehydration was induced by gradually introducing a solution of ethanol and infiltration with increasing concentrations of LR white resin (Delta Microscopies) diluted in ethanol. Inclusion and polymerization were performed over 24 h at 60° C in capsules with LR white resin in the absence of $O_2$. Thin sections (80 nm) were collected onto 200-mesh carbon grids and visualized with an FEI Tecnai Sphera microscope operating at 200 kV and equipped with a Gatan 4x4k UltraScan CCD camera.

### 4.5 Confocal microscopy

Bacterial cultures were done in the same conditions as described above, but they were incubated with pseudonajide tagged with *FITC. After incubation, cells were washed with saline solution then 3 µL was added to glass slides for confocal analysis. The images were acquired using a Leica SP8 DMI 6000 CS confocal microscope, and ImageJ software was used for image analysis.*

### 4.6 Gene expression analysis

*Quantitative real-time PCR (qRT-PCR) was performed on RNA extracted from bacteria cultured during 4 h with or without 6.25 µM of pseudonajide. Nucleic acids were extracted using TRIzol reagent (Thermo Fisher) following the manufacturer's protocol. RNAse-free DNAse I (NEB) was added to 2 µg RNA, then 1 µg RNA was used for reverse transcriptase (RT) reactions with M-MLV reverse transcriptase enzymes*

*(Promega). RT reactions were done using Random Primers (Promega). For the qRT-PCR assay, 10 ng cDNA was used with SYBR Green PCR Master Mix (Applied Biosystems) supplemented with the respective primers (41). The reactions were performed in a StepOne Real-Time system (Thermo Fisher). Expression levels of the 16S rRNA gene were used for the relative gene expression normalization analysis (54). The primers used in this work are listed in Table below. (see Table 1 in the Supplementary Files)*

### 4.7 Toxicity test

Cytotoxicity tests were performed on the ImPACcell robotic platform (BIOSIT, Université de Rennes 1). This featured high-throughput multiparameter image analysis, with both high-content screening and high-content analysis. The platform is equipped with an Olympus microscope and Compix SimplePCI software; a Zeiss Axio Imager M1 microscope with a Zeiss camera and AxioVision software; and imaging systems including an ArrayScan VTI Cellomics reader (Thermo Fisher), Hamilton STARlet and NIMBUS workstations, and a Scienion spotter. Cells used in the test were obtained from an already-existing collection available at BIOSIT (https://biosit.univ-rennes1.fr/impaccell-imagerie-pour-analyse-du-contenu-cellulaire). For the tests, seven different cell lines were used: human hepatocellular carcinoma (HuH7); colorectal adenocarcinoma (Caco-2); breast adenocarcinoma (MDA-MB231); colorectal carcinoma (HCT116); prostatic adenocarcinoma (PC3); lung carcinoma (NCL-H727); and breast cancer (MCF7). The residual cell percentages reported correspond to viable cells compared to the average viable cells in the DMSO control. Viability of 100% represents no cytotoxicity or inhibition of cell growth, while under 25-30% is considered cytotoxic and 0% represents acute cytotoxicity.

## List Of Abbreviations

**AMPs** antimicrobial peptides

**APD** Antimicrobial Peptide Database

**CFU** colony-forming units

**DAG** diacylglycerol

**DMSO** dimethyl sulfoxide

**FITC** fluorescein isothiocyanate

**qRT-PCR** quantitative real-time PCR

**RT** reverse transcriptase

**SEM** scanning electron microscopy

**TEM** transmission electron microscopy

**TSB** tryptic soy broth

# Declarations

### Ethics approval and consent to participate

Not applicable.

### Consent for publication

Not applicable.

### Availability of data and material

The datasets used and/or analysed during the current study available from the corresponding author on reasonable request.

### Competing interests

The authors declare no competing of interests.


### Funding

This study was supported by the Brazilian *Coordenação de Aperfeiçoamento de Pessoal de Nível Superior* (CAPES) (Finance Code 001); *Conselho Nacional de Desenvolvimento Científico e Tecnológico* (CNPq); *Fundação de Amparo à Pesquisa do Estado do Rio Grande do Sul* (FAPERGS-PRONEN) and by the French *Centre National de Recherche Scientifique* (CNRS). The funders had no role in study design, data collection and analysis, decision to publish, or preparation of the manuscript.


### Authors contribution

ROS, MPB, RGVB, SC, RG and AJM designed the experiments; ROS and MPB performed the experiments and analyzed the results; SC performed the electronic microscopy experiments and analysis; ROS and RGVB performed the confocal microscopy experiments and analysis; ROS, MPB, RG and AJM wrote the main manuscript text. All authors agreed to this publication.


### Acknowledgements

Thanks to Emmanuel Giudice and Daniel Thomas for their support in analyzing the results and for discussions about the experimental protocols. Thanks to Juliana Berland for English review


# References


1. Casewell NR, Wüster W, Vonk FJ, Harrison RA, Fry BG. Complex cocktails: the evolutionary novelty of venoms. Trends Ecol Evol. 2013;28(4):219-29.

2. Primon-Barros M, José Macedo A. Animal Venom Peptides: Potential for New Antimicrobial Agents. Curr Top Med Chem. 2017;17(10):1119-56.
3. Wang G, Li X, Wang Z. APD3: the antimicrobial peptide database as a tool for research and education. Nucleic Acids Res. 2016;44(D1):D1087-93.
4. Hancock RE, Diamond G. The role of cationic antimicrobial peptides in innate host defences. Trends Microbiol. 2000;8(9):402-10.
5. Andrea A, Molchanova N, Jenssen H. Antibiofilm Peptides and Peptidomimetics with Focus on Surface Immobilization. Biomolecules. 2018;8(2).
6. Fjell CD, Hiss JA, Hancock RE, Schneider G. Designing antimicrobial peptides: form follows function. Nat Rev Drug Discov. 2011;11(1):37-51.
7. Guilhelmelli F, Vilela N, Albuquerque P, Derengowski LaS, Silva-Pereira I, Kyaw CM. Antibiotic development challenges: the various mechanisms of action of antimicrobial peptides and of bacterial resistance. Front Microbiol. 2013;4:353.
8. Batoni G, Maisetta G, Esin S. Antimicrobial peptides and their interaction with biofilms of medically relevant bacteria. Biochim Biophys Acta. 2016;1858(5):1044-60.
9. Büttner H, Mack D, Rohde H. Structural basis of Staphylococcus epidermidis biofilm formation: mechanisms and molecular interactions. Front Cell Infect Microbiol. 2015;5:14.
10. Flemming HC, Wingender J. The biofilm matrix. Nat Rev Microbiol. 2010;8(9):623-33.
11. Davies D. Understanding biofilm resistance to antibacterial agents. Nat Rev Drug Discov. 2003;2(2):114-22.
12. Donlan RM. Biofilms: microbial life on surfaces. Emerg Infect Dis. 2002;8(9):881-90.
13. Hoyos-Nogués M, Gil FJ, Mas-Moruno C. Antimicrobial Peptides: Powerful Biorecognition Elements to Detect Bacteria in Biosensing Technologies. Molecules. 2018;23(7).
14. Riool M, de Breij A, Drijfhout JW, Nibbering PH, Zaat SAJ. Antimicrobial Peptides in Biomedical Device Manufacturing. Front Chem. 2017;5:63.
15. Byrd AL, Belkaid Y, Segre JA. The human skin microbiome. Nat Rev Microbiol. 2018;16(3):143-55.
16. Nguyen TH, Park MD, Otto M. Host Response to. Front Cell Infect Microbiol. 2017;7:90.
17. Rogers KL, Fey PD, Rupp ME. Coagulase-negative staphylococcal infections. Infect Dis Clin North Am. 2009;23(1):73-98.
18. Rupp ME, Fey PD, Heilmann C, Götz F. Characterization of the importance of Staphylococcus epidermidis autolysin and polysaccharide intercellular adhesin in the pathogenesis of intravascular catheter-associated infection in a rat model. J Infect Dis. 2001;183(7):1038-42.
19. Zimmerli W, Trampuz A, Ochsner PE. Prosthetic-joint infections. N Engl J Med. 2004;351(16):1645-54.
20. Le KY, Park MD, Otto M. Immune Evasion Mechanisms of. Front Microbiol. 2018;9:359.
21. Maki DG, Kluger DM, Crnich CJ. The risk of bloodstream infection in adults with different intravascular devices: a systematic review of 200 published prospective studies. Mayo Clin Proc.

2006;81(9):1159-71.

22. Wang A, Athan E, Pappas PA, Fowler VG, Olaison L, Paré C, et al. Contemporary clinical profile and outcome of prosthetic valve endocarditis. JAMA. 2007;297(12):1354-61.
23. Silva LN, Zimmer KR, Macedo AJ, Trentin DS. Plant Natural Products Targeting Bacterial Virulence Factors. Chem Rev. 2016;116(16):9162-236.
24. Thompson JD, Gibson TJ, Plewniak F, Jeanmougin F, Higgins DG. The CLUSTAL_X windows interface: flexible strategies for multiple sequence alignment aided by quality analysis tools. Nucleic Acids Res. 1997;25(24):4876-82.
25. Chang CY. Surface Sensing for Biofilm Formation in. Front Microbiol. 2017;8:2671.
26. Kirchhoff C, Cypionka H. Propidium ion enters viable cells with high membrane potential during live-dead staining. J Microbiol Methods. 2017;142:79-82.j
27. Malanovic N, Lohner K. Gram-positive bacterial cell envelopes: The impact on the activity of antimicrobial peptides. Biochim Biophys Acta. 2016;1858(5):936-46.
28. Omardien S, Drijfhout JW, Vaz FM, Wenzel M, Hamoen LW, Zaat SAJ, et al. Bactericidal activity of amphipathic cationic antimicrobial peptides involves altering the membrane fluidity when interacting with the phospholipid bilayer. Biochim Biophys Acta. 2018.
29. Peschel A, Sahl HG. The co-evolution of host cationic antimicrobial peptides and microbial resistance. Nat Rev Microbiol. 2006;4(7):529-36.
30. Devocelle M. Targeted antimicrobial peptides. Front Immunol. 2012;3:309.
31. Mandal SM, Roy A, Ghosh AK, Hazra TK, Basak A, Franco OL. Challenges and future prospects of antibiotic therapy: from peptides to phages utilization. Front Pharmacol. 2014;5:105.
32. Lázár V, Martins A, Spohn R, Daruka L, Grézal G, Fekete G, et al. Antibiotic-resistant bacteria show widespread collateral sensitivity to antimicrobial peptides. Nat Microbiol. 2018;3(6):718-31.
33. Ageitos JM, Sánchez-Pérez A, Calo-Mata P, Villa TG. Antimicrobial peptides (AMPs): Ancient compounds that represent novel weapons in the fight against bacteria. Biochem Pharmacol. 2017;133:117-38.
34. Kang HK, Kim C, Seo CH, Park Y. The therapeutic applications of antimicrobial peptides (AMPs): a patent review. J Microbiol. 2017;55(1):1-12.
35. Toke O. Antimicrobial peptides: new candidates in the fight against bacterial infections. Biopolymers. 2005;80(6):717-35.
36. Nguyen LT, Haney EF, Vogel HJ. The expanding scope of antimicrobial peptide structures and their modes of action. Trends Biotechnol. 2011;29(9):464-72.
37. Falcao CB, de La Torre BG, Pérez-Peinado C, Barron AE, Andreu D, Rádis-Baptista G. Vipericidins: a novel family of cathelicidin-related peptides from the venom gland of South American pit vipers. Amino Acids. 2014;46(11):2561-71.
38. Neuhaus FC, Baddiley J. A continuum of anionic charge: structures and functions of D-alanyl-teichoic acids in gram-positive bacteria. Microbiol Mol Biol Rev. 2003;67(4):686-723.

39. Weidenmaier C, Peschel A. Teichoic acids and related cell-wall glycopolymers in Gram-positive physiology and host interactions. Nat Rev Microbiol. 2008;6(4):276-87.
40. Saar-Dover R, Bitler A, Nezer R, Shmuel-Galia L, Firon A, Shimoni E, et al. D-alanylation of lipoteichoic acids confers resistance to cationic peptides in group B streptococcus by increasing the cell wall density. PLoS Pathog. 2012;8(9):e1002891.
41. García-Gómez E, Miranda-Ozuna JFT, Díaz-Cedillo F, Vázquez-Sánchez EA, Rodríguez-Martínez S, Jan-Roblero J, et al. Staphylococcus epidermidis lipoteichoic acid: exocellular release and ltaS gene expression in clinical and commensal isolates. J Med Microbiol. 2017;66(7):864-73.
42. Gründling A, Schneewind O. Genes required for glycolipid synthesis and lipoteichoic acid anchoring in Staphylococcus aureus. J Bacteriol. 2007;189(6):2521-30.
43. Gründling A, Schneewind O. Synthesis of glycerol phosphate lipoteichoic acid in Staphylococcus aureus. Proc Natl Acad Sci U S A. 2007;104(20):8478-83.
44. Zhang LJ, Gallo RL. Antimicrobial peptides. Curr Biol. 2016;26(1):R14-9.
45. Gruenheid S, Le Moual H. Resistance to antimicrobial peptides in Gram-negative bacteria. FEMS Microbiol Lett. 2012;330(2):81-9.
46. Joo HS, Fu CI, Otto M. Bacterial strategies of resistance to antimicrobial peptides. Philos Trans R Soc Lond B Biol Sci. 2016;371(1695).
47. Foschiatti M, Cescutti P, Tossi A, Rizzo R. Inhibition of cathelicidin activity by bacterial exopolysaccharides. Mol Microbiol. 2009;72(5):1137-46.
48. Heilmann C. Adhesion mechanisms of staphylococci. Adv Exp Med Biol. 2011;715:105-23.
49. Hussain M, Heilmann C, Peters G, Herrmann M. Teichoic acid enhances adhesion of Staphylococcus epidermidis to immobilized fibronectin. Microb Pathog. 2001;31(6):261-70.
50. Jabbouri S, Sadovskaya I. Characteristics of the biofilm matrix and its role as a possible target for the detection and eradication of Staphylococcus epidermidis associated with medical implant infections. FEMS Immunol Med Microbiol. 2010;59(3):280-91.
51. Von Borowski RG, Macedo AJ, Gnoatto SCB. Peptides as a strategy against biofilm-forming microorganisms: Structure-activity relationship perspectives. Eur J Pharm Sci. 2018;114:114-37.
52. Antunes AL, Trentin DS, Bonfanti JW, Pinto CC, Perez LR, Macedo AJ, et al. Application of a feasible method for determination of biofilm antimicrobial susceptibility in staphylococci. APMIS. 2010;118(11):873-7.
53. Trentin DaS, Giordani RB, Zimmer KR, da Silva AG, da Silva MV, Correia MT, et al. Potential of medicinal plants from the Brazilian semi-arid region (Caatinga) against Staphylococcus epidermidis planktonic and biofilm lifestyles. J Ethnopharmacol. 2011;137(1):327-35.
54. Livak KJ, Schmittgen TD. Analysis of relative gene expression data using real-time quantitative PCR and the 2(-Delta Delta C(T)) Method. Methods. 2001;25(4):402-8.

# Tables

Due to technical limitations Table 1 is available as a download in the Supplementary Files.

# Additional File Legends

**S1. Antibiofilm formation activity screening of 14 short peptides in *S. epidermidis*.** Graphs showing biofilm mass quantification at an optical density of 570 nm ($OD_{570}$) using the crystal violet protocol (light gray), and growth at $OD_{600}$ (dark gray), in the presence of different concentration of 14 peptides. TSB culture medium with 2% dimethyl sulfoxide (DMSO) was used as a control for biofilm formation and growth, and rifampicin was the antibiofilm and antibiotic positive control. $OD_{600}$ was measured at time zero and at 24 h for growth normalization.

**S2. Antibiofilm formation testing of 16 short peptides in *Pseudomonas aeruginosa*.** Graphs demonstrating biofilm mass quantification at $OD_{570}$ by the crystal violet protocol (left) and growth at $OD_{600}$ (right) in the presence of different concentrations of 16 peptides. Tests were performed over 24 h. Gentamicin was used as the antibiofilm and antibiotic control, while TSB culture medium and TSB containing 2% DMSO were used as biofilm formation and growth controls.

# Figures

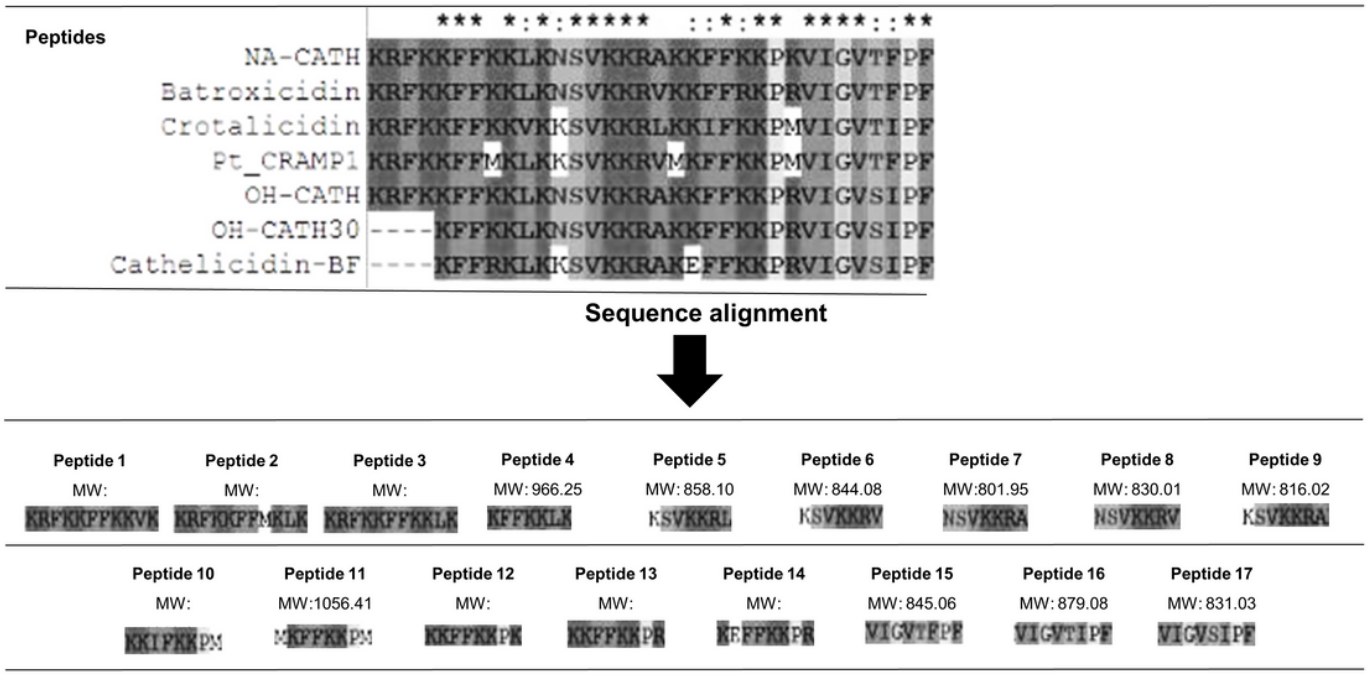


**Figure 1**

Peptide alignment and selection of short molecules. (Top) Chart demonstrating the sequence alignment of seven peptides derived from snake venom. (Bottom) After analysis with Clustal X software (24), 17

small sequences were selected for antibiofilm testing. The figure shows each short peptide's respective molecular weight (MW).

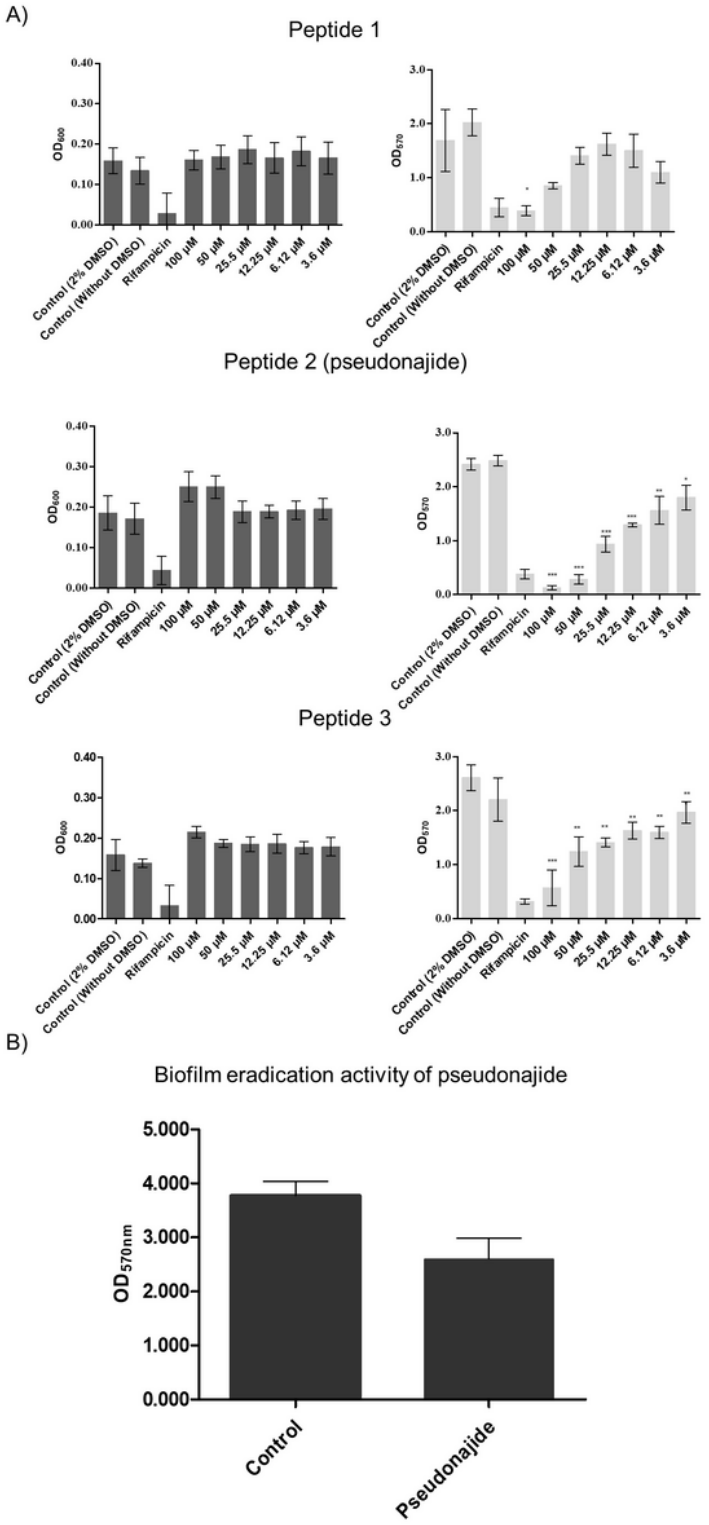


## Figure 2

Antibiofilm and biofilm eradication activity. (A) Antibiofilm formation (left graphs) and bacterial growth (right graphs) after 24 h of exposition to different concentrations of peptide 1, peptide 2 (pseudonajide), and peptide 3. S. epidermidis ATCC 35984 cell suspension was incubated alone or in the presence of

decreasing concentrations of peptides. An adapted crystal violet protocol was used for biomass measurement at optical density of 570 nm (OD570) (53), and growth analysis was done at an optical density of 600 nm (OD600). Culture medium with 2% dimethyl sulfoxide (DMSO), only culture medium was used as growth control, while rifampicin was the antibiofilm positive control. OD600 was measured at time zero and at 24 h for growth normalization. (B) The biofilm eradication activity of peptide 2, pseudonajide (bottom graph) was measured by adding 25 μM of pseudonajide in pre-formed biofilm and incubating for more 24 h. All the tests were performed with at least with 3 different biological replicates each including at least 3 technical replicates. Error bars are shown, and statistical analysis was performed using Student's t-test, where: *, $p < 0.05$; **, $p < 0.01$; ***, $p < 0.001$.

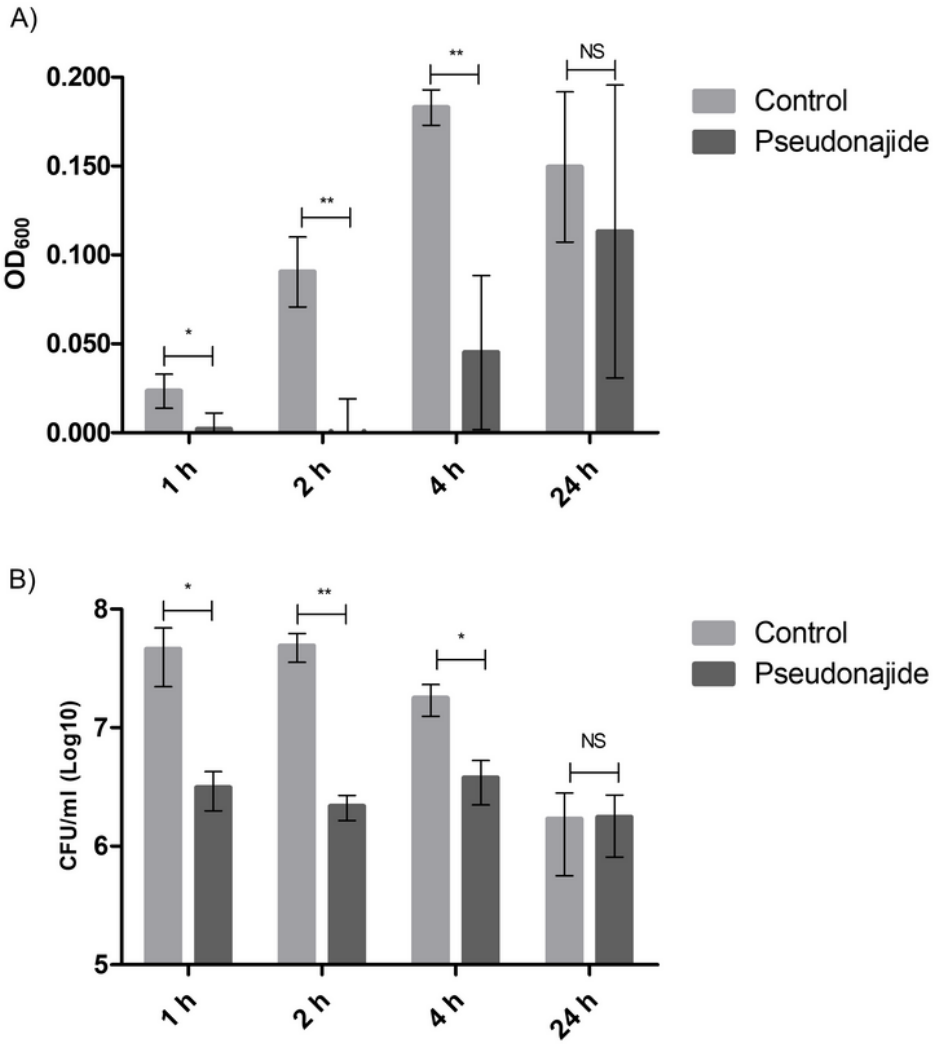


## Figure 3

Antimicrobial activity of peptide 2. Staphylococcus epidermidis was cultured in the same conditions as the biofilm tests, but with a different pseudonajide concentration (25 μM). (A) Optical density measurements at 600 nm (OD600) show a reduction in bacterial growth in the presence of 25 μM peptide 2 after 1, 2, and 4 h. (B) Colony-forming unit (CFU) testing confirmed the reduction in cell viability as compared to the control. All the tests were performed with at least 3 different biological replicates, each

having at least 3 technical replicates. Error bars are shown, and statistical analysis was performed applying Student's t-test, where: *, $p < 0.05$; **, $p < 0.005$; NS, non-significant.

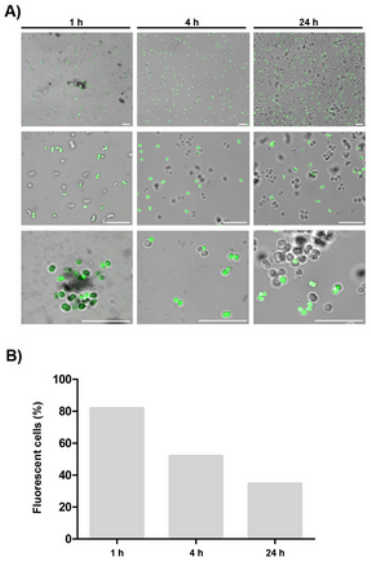


## Figure 4

Pseudonajide is located in the cell envelope and inside the bacterial cell. (A) Confocal microscopy images of Staphylococcus epidermidis incubated for 1, 4, and 24 h with 25 μM pseudonajide tagged with fluorescein isothiocyanate (FITC). Scale, 10 μm. Cells were washed once with saline solution, and 3 μL

cell suspension was added to each glass slide. (B) Graph demonstrating the percentage of cells that were fluorescent at each time point. Shown are 5 random fields, with approximately 1,000 cells counted for each time point. The percentage was calculated by dividing the total number of cells in the field by the number of cells that presented fluorescence. Images were analyzed using Fiji software.

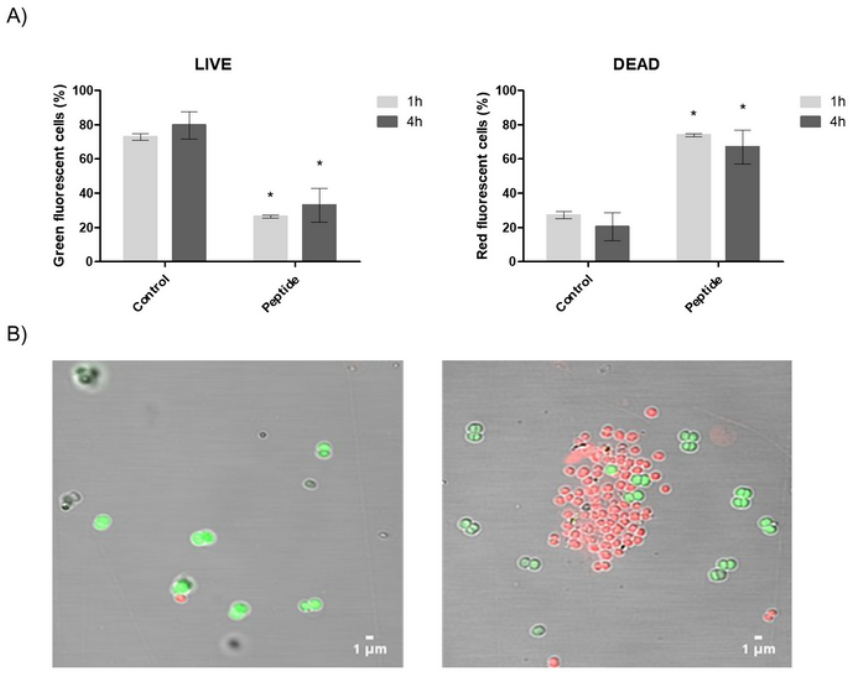


## Figure 5

LIVE/DEAD experiments in the presence of pseudonajide. (A) Confocal microscopy images showing cells (left) unexposed and (right) exposed to the molecule after incubation cells were treated with LIVE/DEAD BacLight reagent (Thermo Fisher). (B) Graph of the percentages of DEAD (red) and LIVE (green) cells. At least 1,000 cells were counted in more than 10 randomly chosen fields per condition, and the experiments were performed in triplicate for each time point. Bars represent the standard deviation. Statistical analysis comparing results to the respective control conditions (Student's t-test): *, $p < 0.05$.

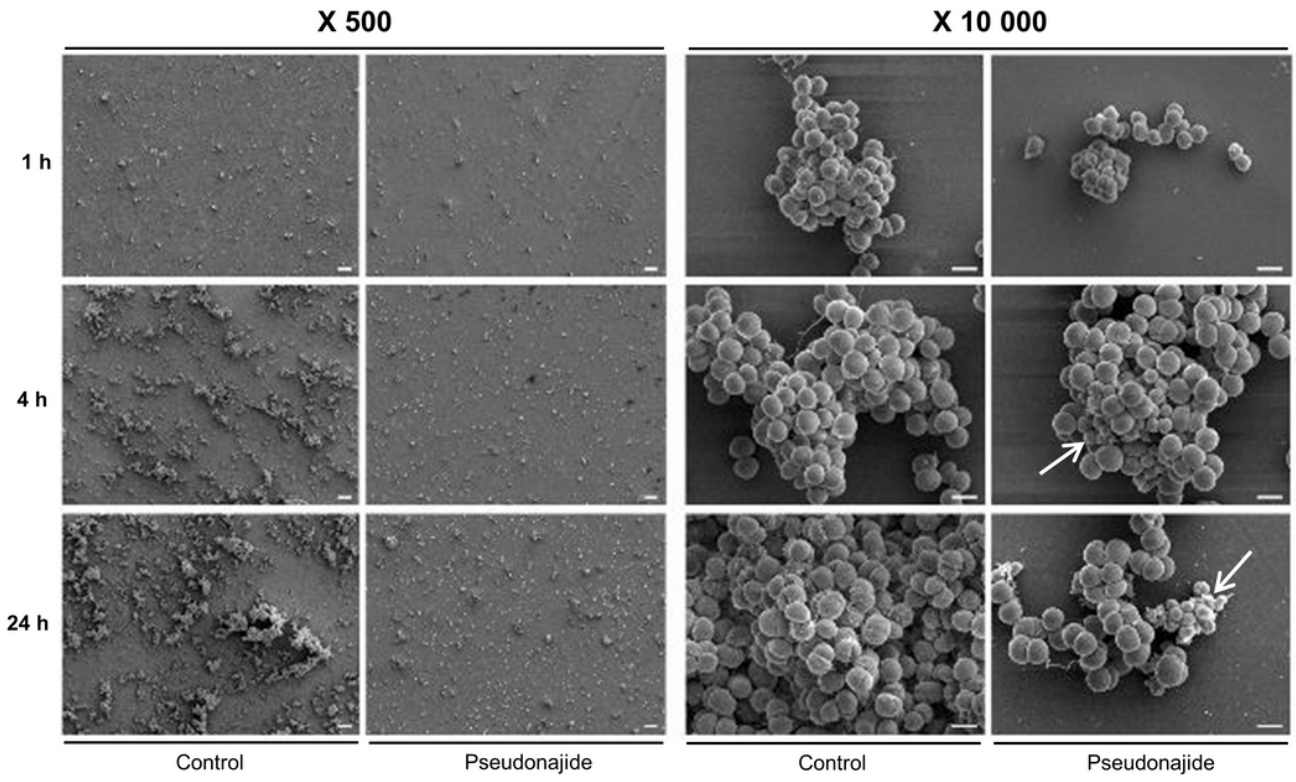


## Figure 6

Scanning electron microscopy images of Staphylococcus epidermidis in the presence and absence of pseudonajide. Bacterial cells were cultured with or without 25 μM peptide 2 (pseudonajide) for 1, 4, and 24 h. Plastic slides were placed inside the culture well plates and used to analyze biofilm and cell morphology. White arrows indicate the cells with different morphologies at 4 and 24 h in the presence of pseudonajide. Images are shown at 500 and 10,000x magnifications, and were obtained using a JEOL JSM-7100F scanning electron microscope.

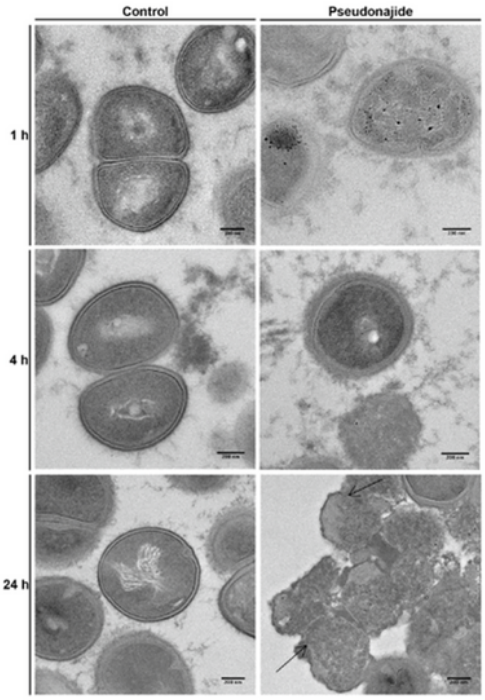


## Figure 7

Transmission electron microscopy images of Staphylococcus epidermidis in the presence or absence of pseudonajide. S. epidermidis cells were cultured with or without 25 μM of the peptide and imaged at three different time points. Cells were detached from the well plate using disposable tips, and all content was treated following the TEM protocol (Materials and Methods). Dark arrows indicate cell wall defects and membrane disruption in the presence of pseudonajide. Scale bars, 200 nm.

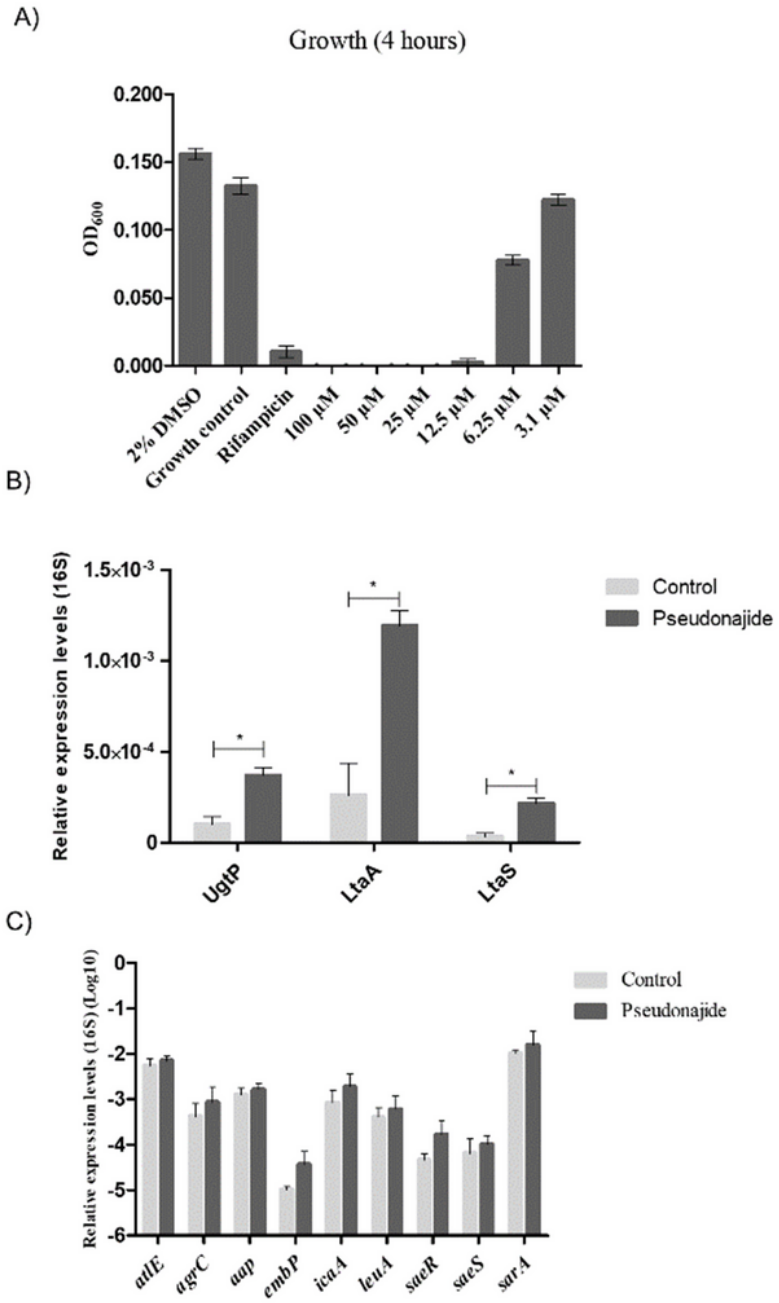


## Figure 8

Gene expression analysis. Graphs of gene expression analysis for three genes coding for the lipoteichoic acid assembly cascade. (A) Bacterial growth after 4 h exposition to different concentrations of peptide 2, pseudonajide. Culture medium with 2% DMSO was used as a control, and rifampicin was the antibiofilm positive control. OD600 was measured at time zero and at 24 h for growth normalization. For gene expression analysis, cDNA was obtained through reverse transcriptase reactions on mRNA extracted from

Staphylococcus epidermidis cultured in the presence (peptide) or absence (control) of 6.25 µM pseudonajide. (B) Expression levels of genes ugtP, ltaA, and ltaS under the same testing conditions. (C) Expression levels of biofilm-related genes under these same conditions. The 2-ΔΔct method was used to normalize expression levels to 16S rRNA (54). All tests were performed in at least 3 different biological replicates each having at least 3 technical replicates. Error bars are shown, and statistical analysis was performed using Student's t-test, where: *, $p < 0.05$.

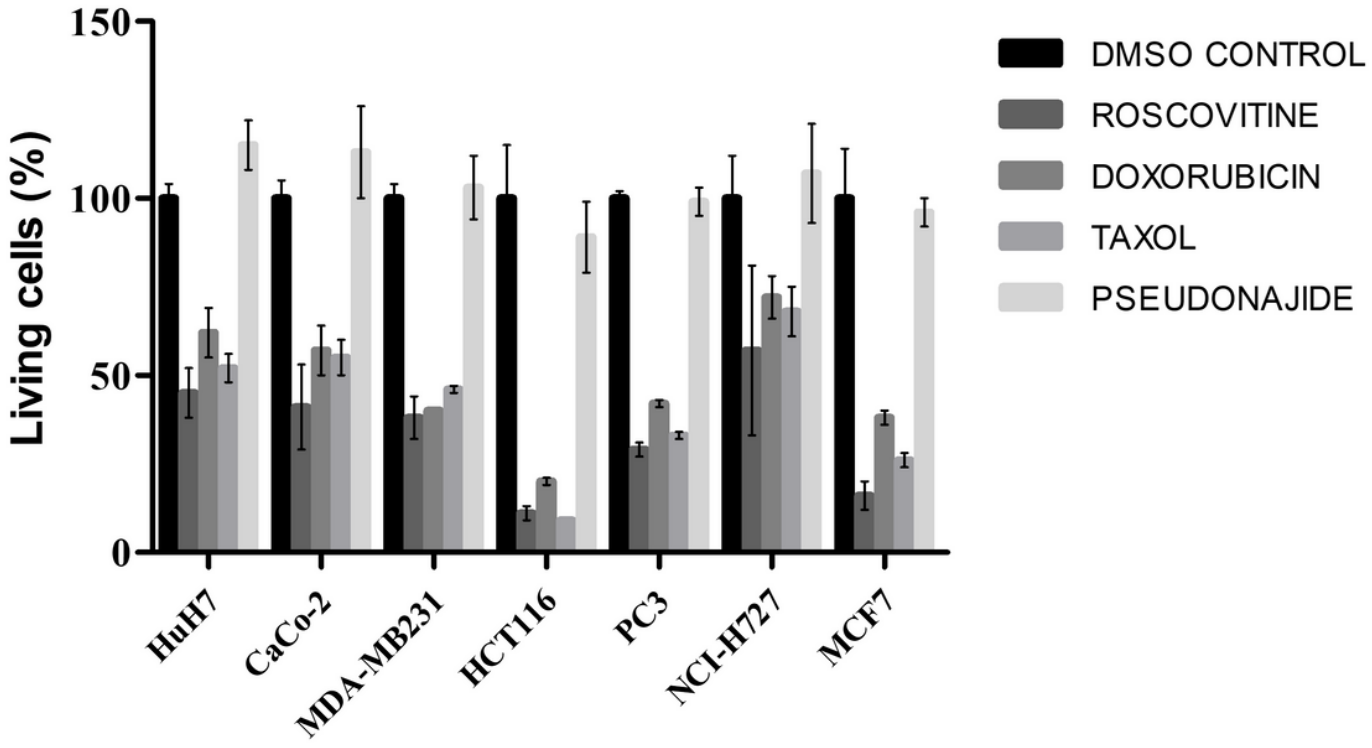


## Figure 9

Evaluation of pseudonajide cytotoxicity. Graph demonstrating the percentage of living cells after 24 h exposition to 25 µM of each peptide. For the tests, seven different human cell lines were used. For comparison, the number of living cells in the DMSO control was considered as 100%, and the three cytotoxic drugs roscovitine, doxorubicin, and taxol were used as positive controls. All tests were performed at the ImPACcell automatized platform of cytotoxicity evaluation (Université de Rennes 1).

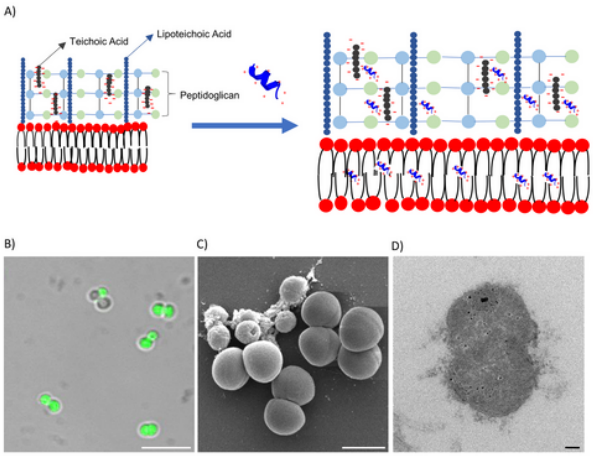


**Figure 10**

Proposed mechanism of action for peptide 2. (A) Schematic of the proposed mechanism of action of pseudonajide in the cell walls and membranes of Gram-positive bacteria. The cationic peptide is shown interacting with negative charges from the cell wall components and with the hydrophobic portions of bacterial membranes. Such interactions lead to: (B) cell envelope binding, shown in a confocal microscopy image; (C) defective morphology, observed by scanning electron microscopy; and (D) cell wall and membrane fractures, observed by transmission electron microscopy.

# Supplementary Files

This is a list of supplementary files associated with this preprint. Click to download.

- SupplementalS1Macedo.tif
- Table1.jpg
- SuplementalS2Macedo.tif